

New Functionalities in “SINDBAD” Software for Realistic X-Ray Simulation Devoted to Complex Parts Inspection

Joachim TABARY, Françoise MATHY, Patrick HUGONNARD, CEA-LETI, Grenoble,
France

Abstract. In NDT studies, the availability of a radiographic devices simulation is of primary interest to design the most suitable system and to predict the future device performance. Numerical simulation of radiographs and CT scans makes inspections more reliable and efficient by providing realistic quantitative answers to non-trivial non-destructive evaluations of complex components.

In this context, the X-ray radiographic simulation software, Sindbad, has been developed in our laboratory. This software can model any radiographic set-up, including the X-ray source, the beam interaction (direct and scattered) inside the object represented by its CAD model, and the imaging process in the detector (different types). For each step of the virtual experimental bench, Sindbad combine different modelling modules, accessed via Graphical User Interfaces, to provide realistic synthetic images. In this paper, we present the new functionalities which have been recently integrated in Sindbad to improve the simulation of radiographs of complex parts including defects, under specific and typical configurations.

First of all, the interface of the new version of BRL-CAD allows the operator to insert easily flaws of various shapes, sizes, and materials within the CAD representation of the part. Moreover, as Sindbad raytracing functions called for the computing of the direct image have been adapted for small details projection, Sindbad can now efficiently compute realistic radiographs of small defects included in complex parts. Some geometric improvements have also been recently integrated: the modelling of panoramic sources, curved detectors and the possibility to place the detector inside the object. Concerning scattered modelling, the Monte Carlo code has been accelerated in cases of low stopping power detectors, like films. Finally, the new version of Sindbad contains a new model of detector: the cascaded system model which is especially useful for flat panel detectors.

Introduction

In the context of NDT studies, X-ray simulation tools are of primary interest during the design stage of radiographic facilities, when they can help to choose the device parameters (X-ray tube settings such as voltage and filtration, detector type and thickness, geometry of the bench, etc.) and predict performances of the future device. Several teams involved in X-ray NDE simulation [1, 2, 3, 4, 5] have developed their own software, based on analytical or Monte Carlo models and using ray tracing techniques, computer aided design (CAD) of the examined sample, and a graphical user interface (GUI).

The X-ray radiographic simulation software, Sindbad [6, 7, 8, 9], has been developed to help the design stage of radiographic systems or to evaluate the efficiency of image processing techniques, in both medical imaging and Non-Destructive Evaluation (NDE)

industrial fields. In this paper we give an overview of Sindbad and present the recent evolutions for simulation of radiographs of complex parts including defects.

1. Overview of Sindbad [6]

The physics of the radiographic inspection process can be divided into three separate parts, namely the X-ray beam generation in the source, the beam interaction with the examined sample, and the imaging process (detection of the remaining photon flux and transformation into a measured signal) as shown on Figure 1.

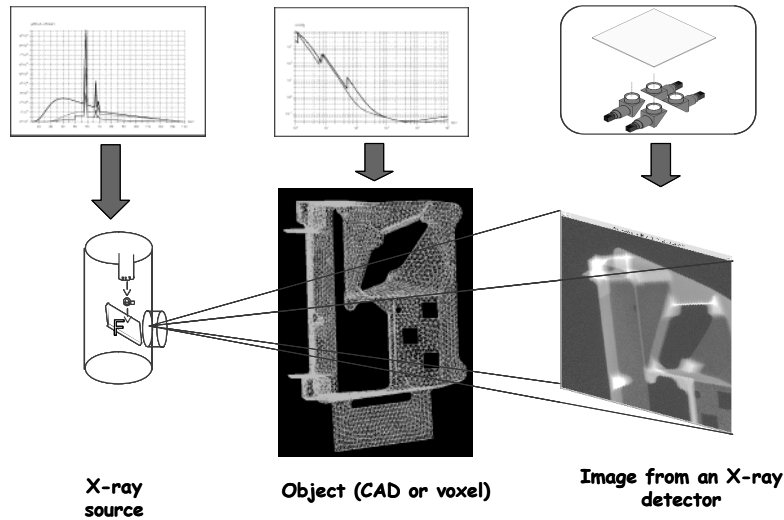


Figure 1 : Sindbad architecture.

1.1 Source modelling

The implemented X-ray tube model, which can be used between 30 and 450 kV, simulates the physical phenomena involved in bremsstrahlung and characteristic photon production with a semi-empiric model. It takes into account the anode angle and composition, the inherent and additional filtration and the photon exit angle. Experiments performed at LETI show that the calculated and measured doses usually agree to within 20%. Tabulated spectra can also be used.

1.2 Detector modelling

Detectors are modelled in two successive steps. The first step which is common to all types of detectors computes the energy deposition in the sensing part of the detector using the energy absorption attenuation coefficients. The second step, specific to each type of detector, simulates the successive physical phenomena involved in the energy to signal transformation. Several models have been developed for specific detectors as scintillating screen viewed by a CCD camera, radiographic film.

1.3 Interaction simulation

Concerning the interaction in the object, the first approach adopted was an analytical one which combines ray tracing techniques and the attenuation law (Beer Lambert) by calculating the energy dependent attenuation due to the crossed materials. The 3D analytical simulation computes an image of the uncollided flux simulation which relies on the computation of the attenuation of the incident flux, binned in narrow energy channels, by the examined sample. This computing model shows very efficient results concerning the uncollided photon flux but fails to evaluate the scattered photon flux correctly.

A Monte Carlo simulation module [7] has also been implemented in Sindbad in order to compute the radiation scattered in the examined object. It relies on a coupling of the BRL-CAD CAD and ray-tracing package [10] with EGS-NOVA [11], a program dedicated to Monte Carlo radiation transport simulation. This Monte Carlo method gives good quality results either for uncollided or scattered photon flux images but its use is largely limited by the execution time drawback.

An original model was developed then, combining the advantages of both analytical and Monte Carlo techniques [8]. The purpose of this computing model is to provide a total synthetic radiograph by combining images obtained from two simulations, one performed with the analytical model for the uncollided photon flux and the other one with the Monte Carlo model for the scattered radiation. As presented in the scheme in Figure 2, the absorbed energy Monte Carlo scattered flux image estimated for a low dose is scaled up to the analytical dose level, and then combined to the uncollided flux image. This scaling is independently performed for both the mean scattered image and the scattered noise image. The main advantage of this combination mode is that it becomes possible to obtain detailed simulated images, taking into account various interaction effects such as scattered, in a feasible computation time. This module has been recently improved by developments [9] to accelerate calculation (simplification of object) and to enable more geometrical configurations (curved detector, panoramic source and backscattered).

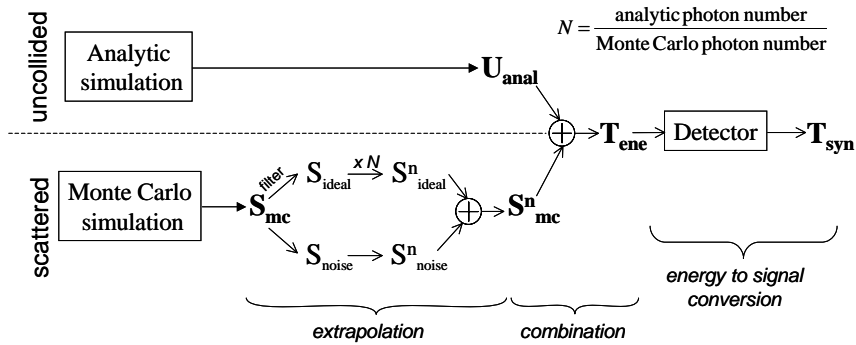


Figure 2 : Analytical and Monte Carlo images combination scheme.

2. Acceleration of the scattered simulation in case of low stopping detector

2.1 Method

Concerning estimation of the scattered flux by extrapolation of the Monte Carlo computed images, we faced to a problem of calculation speed in case of detectors with a very poor detection efficiency, as a radiographic film. Indeed, under typical conditions, it appears that the detection efficiency of a film can be under 1%. As the attenuation due to the part can be

quite significant, it induces that sometimes, less than 1 photon over about 25 000 emitted by the source both scatters in the object and is detected by the sensitive part of the film. In Monte Carlo computation, the number of pixels is a good approximation of the number of detected photons necessary to have a good estimation of the scattered image. Consequently, sometimes, it would be necessary to emit about $1e10$ photons in the Monte Carlo simulation, which would probably take several days of computing time.

The solution we applied to avoid this problem is to compute the Monte Carlo scattered image (energy image) as if the film was ideal, that is to say detecting all the photons. Therefore, we apply on these resulting images a mean energy detection efficiency factor, computed during the Monte Carlo computation, to recover the good scattered image level (Figure 3 for illustration). This process has to be performed both with the mean scattered image and the noise variance one, to assure a good level of noise. This method is similar to a reduction variance method as we force photons to be absorbed in the sensitive part of the detector. The gain in calculation time is directly linked to the detection factor.

It is clear that the absorption process does not act in a similar way for the mean scattered image and the corresponding noise variance image. Thus, we must study exactly what happens when the extrapolation process is applied on the incident image, rather than on the absorbed one.

When considering the mean scattered image (noted S_{ideal} in Figure 2), if we call E_{abs} and E_{inc} respectively the total energy of absorbed and incident photons in the detector, we have:

$$E_{abs} = \int_{spect} E.N_{abs}(E)dE = \int_{spect} E.e^{-\mu_{tot}(E)l} N_{inc}(E)dE = \left\langle e^{-\mu_{tot}(E)l} \right\rangle_1^{mean} \times E_{inc}$$

$$\text{with } \left\langle e^{-\mu_{tot}(E)l} \right\rangle_1^{mean} = \frac{\int_{spect} E.N_{abs}(E)dE}{\int_{spect} E.N_{inc}(E)dE} = \frac{E_{abs}}{E_{inc}} = \eta_1^{abs} \quad \text{representing the mean absorption}$$

coefficient, integrated under the spectrum and considering the energies and not the photons. This coefficient can be easily computed by cumulating incident and absorbed energies during the Monte Carlo calculation.

When considering the noise variance image (noted S_{noise} in Figure 2), we have :

$$\begin{aligned} Var(E_{abs}) &= Var\left(\int_{spect} E.N_{abs}(E)dE\right) = \int_{spect} E^2.Var(N_{abs}(E))dE \\ &= \int_{spect} E^2.N_{abs}(E)dE = \int_{spect} E^2.e^{-\mu_{tot}(E)l} N_{inc}(E)dE = \left\langle e^{-\mu_{tot}(E)l} \right\rangle_2^{mean} \times Var(E_{inc}) \end{aligned}$$

$$\text{with } \left\langle e^{-\mu_{tot}(E)l} \right\rangle_2^{mean} = \frac{\int_{spect} E^2.N_{abs}(E)dE}{\int_{spect} E^2.N_{inc}(E)dE} = \eta_2^{abs}. \quad \text{Consequently, the correcting factor } \eta_2^{abs} \text{ to}$$

apply on the noise variance image is different from the one η_1^{abs} applied for the mean scattered image. However, η_2^{abs} can also be easily calculated by cumulating squared incident and absorbed energies during the Monte Carlo calculation.

The user is free to use this new speed-up option when estimating the scattered image, depending on the modelled detector. It is important to note that this method assumes that the stopping power is constant in the entire scattered image, i.e. that the scattered spectrum and the incident angles of scattered photons are similar in the entire image. These assumptions can be assumed for such homogeneous objects. However, to check it, a new

functionality in Monte Carlo simulations has been developed to get the total, direct and scattered spectra in several areas of the detector.

2.2 Validation

The simulations presented in Figure 3 aim at checking if the speed-up method does not induce errors on scattered computation. This figure represents only the method for the mean scattered image but the same process is also achieved on the noise variance image to assure a good level of noise ([12] Deliv.1.7 for more details). The simulated configuration corresponds to a radiograph of a SNECMA stiffener part in nickel based alloy (NC19FeNb) with a Kodak M100 film, whose thickness is 25 μm of AgBr. The parameters of radiography are a voltage of 140kV for the source and a distance between the source and the film (set on the part) of 700mm. The beam is reduced to a cone with an angle aperture of 3.9°, in order to reduce time of calculation of scattered images.

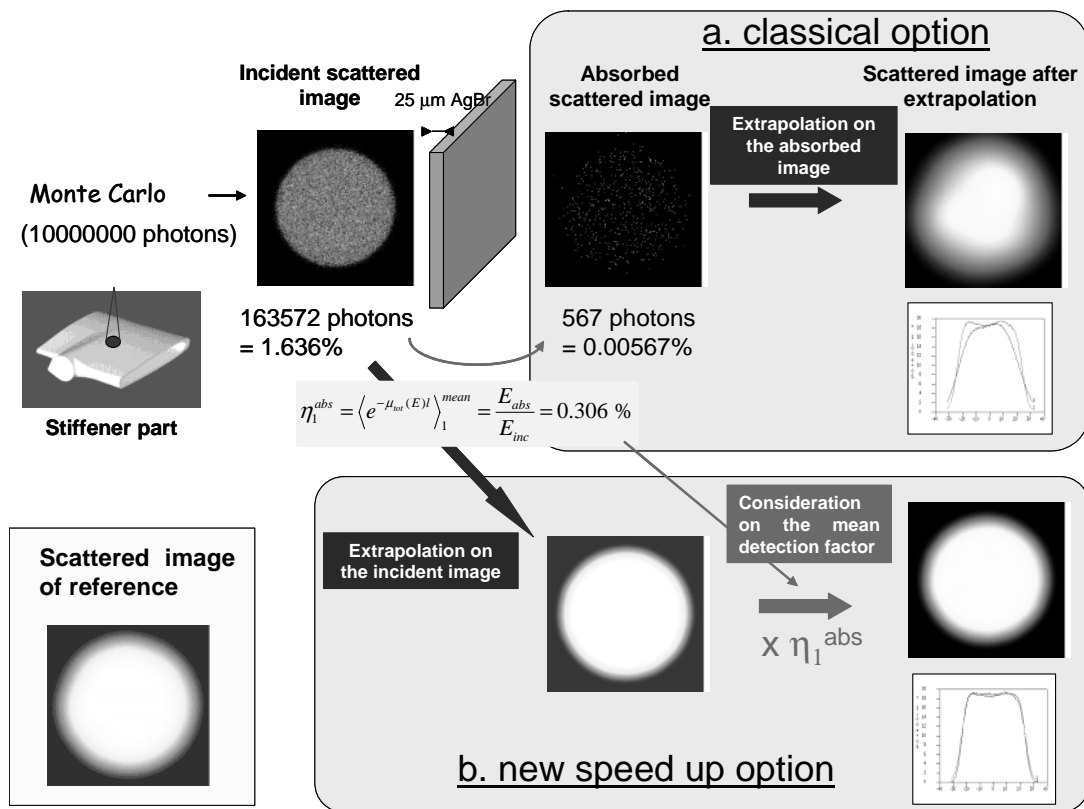


Figure 3 : Scattered image calculation with (b) and without (a) the new speed option, consisting in performing the extrapolation on the incident image rather than on the absorbed one and correcting afterward with a mean detection factor. This figure represents only the method on the mean scattered image but the same process is also achieved on the noise image to assure a good level of noise.

For validation, we first compute a reference scattered image by performing a simulation without using the speed-up option but with a large number of emitted photons: 1e9 Monte Carlo showers. For validation of the speed-up method, a second simulation is performed with 1e7 emitted photons and the extrapolation process is performed two times: the first on the absorbed scattered image (a: classical method) and a second time on the incident scattered image (b: new speed up method). With the classical option, the scattered image is estimated with only 567 photons which have both scattered in the object and been absorbed in the film. Therefore, the extrapolation is not satisfactory and the resulting scattered image is far from the reference one. On the other hand, when using the new speed up option, the

extrapolation is performed on the incident image which presents a better statistic (163572 photons). Finally, the resulted scattered image is closest to the reference scattered image. The validation concerning the noise has been done in a same way. In conclusion, this method looks very efficient to speed up scattered estimation. Its limitation is the estimation of the absorption coefficients which can be very approximate if the number of initial emitted photons is too weak.

3. Simulation of Small Defects in CAD Object

3.1 CAD insertion of defect via BRL-CAD

To be simulated in Sindbad, 3D objects must be described or converted in formats compatible with the BRL-CAD CAD package [10]. Two formats are available: the constructive solid geometrical (CSG) format of BRL-CAD, consisting in combinations (union, subtraction, intersection) of simple geometric shapes (sphere, box, cone...) and the faceted format, resulted from conversion of standard stereolithography (STL) format.

Objects in the BRL-CAD are built according to a simple architecture: they are composed of different regions (with a given material) which are composed of different combinations of CAD items, which can be either simple shapes described in CSG format or in faceted format. BRL-CAD is very flexible as the user can easily add, subtract or modify any item in a given object, even if it is not in the same format. Such modification or creation can be carried out thanks to an interactive GUI interface proposed by BRL-CAD or by command line, for more accuracy and repeatability ([12] Deliv.1.10). Thus, it is very easy to insert a defect inside a BRL-CAD object. This defect can be drawn in BRL-CAD or recovered from a faceted description. Thanks to the GUI interface of BRL-CAD, the user can easily move it, turn it, scale it or even distort it by playing on its control points (Figure 4).

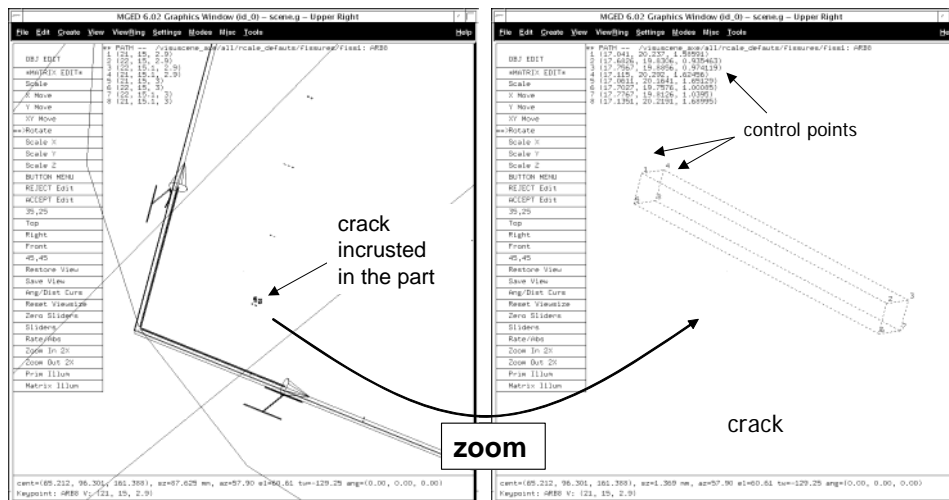


Figure 4 : BRL-CAD interface used to insert defects in CAD models. Many buttons (scale, rotation, move) enable the user to modify the crack which is inserted in the object.

3.2 Over sampling of detector

In Sindbad, the computing of the direct image is performed by tracing rays from the source point to every pixel of the detector through the sample. When the objects have fine structures with characteristic sizes identical or smaller than the width of the pixels, the ray-tracing carried out in Sindbad is not enough dense to cross these small objects.

Consequently, and because traced rays are dimensionless, the structures do not appear on resulting images.

The solution consists in over-sampling the detector so as to refine the grid of rays and thus to increase the probabilities of crossing the fine structures. The more significant the over-sampling is, the more numerous the number of rays crossing the small objects are, which induce a more realistic projection. On the other hand, the computing time is directly related (linear relation) to the number of rays. Once the energy image is calculated, it is obviously necessary to achieve a gathering of pixels to recover the good size of pixels.

For more convenience, we propose to manage the over sampling in an automatic and transparent way for the user. Only one more input parameter must be provided by the user: the characteristic size of the “smallest structures to be projected”. The rate of over sampling is then calculated to assure that at least one ray will cross the so called “smallest structure to be projected” ([12] Deliv.1.10).

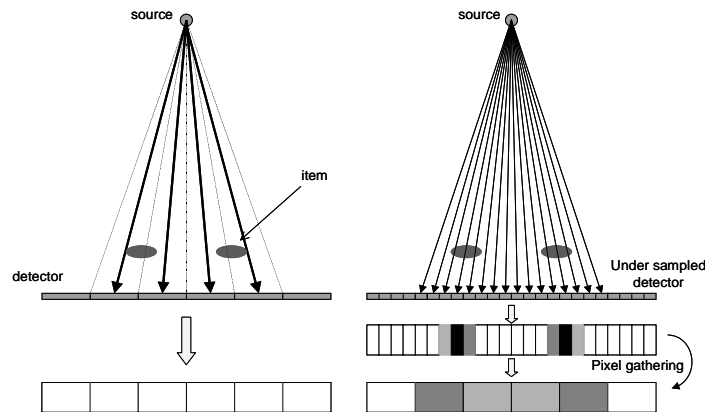


Figure 5 : Scheme of the over sampling process to project small details.

4. A new model of detector : the cascaded system model

4.1 Principle of the method

The model proposed for flat panel detector panel is based on the model described by Rabbani & Cunningham (see [13], [14]), called the cascaded linear system model. This model breaks up the whole detection process into several linear processes. Through each stage, mean signal and noise of the image are propagated according to typical formulae which depend on the kind of the process (amplification process, stochastic blurring process, deterministic blurring process, noise addition process

).The first references of Rabbani & Cunningham present this cascaded linear system model to compute global characteristics of detectors, such as the global MTF (Modulation Transfer Function), the NPS (Noise Power Spectrum) and the DQE (Detective Quantum Efficiency). This model is based on the propagation of the mean signal and the noise characteristic (NPS) through each stage of an imaging detector. However, these data, except the MTF, are difficult to exploit for simulation, especially for the noise modelling.

Bissonnette and Cunningham (see [15], [16], [17]) have adapted this model for simulation purpose, and this is this method which has been developed in Sindbad. Precisely, this model is based on the propagation of the mean image and the noise image through each stage of the detector. Each stage of the detection process is modelled by a linear

mathematical system which transforms the mean image S_{i-1} and the noise image N_{i-1} to new ones S_i and N_i (Figure 6). In the new detector module of Sindbad, the user is free to build its own detector model by cumulating different linear systems, according to the kind of detectors and to its available data. This succession of mathematical boxes assures the conversion of the initial absorbed energy image to the real signal image, expressed in grey levels in most cases. Initial input data of this cascaded system is the mean absorbed energy image S_0 (expressed in keV) and its associated noise image N_0 , both computed analytically by considering the thickness and material of the detector and pixel sizes.

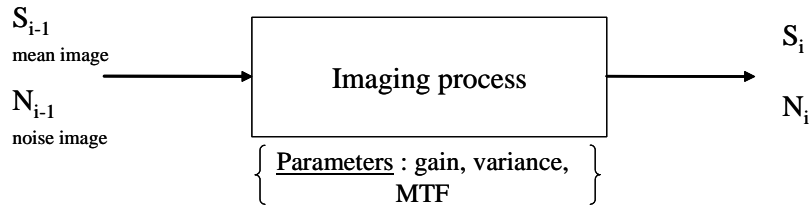


Figure 6 : Input/output principle of linear imaging processes

4.2 The elementary linear processes

In the cascaded linear system model, different elementary linear processes are identified to describe a detector:

- Amplification process

An amplification process is characterized by its gain g and the variance of this gain σ_g , knowing that the amplification is a stochastic process whose certainty is not assured. The effect of the gain on the mean image is simply: $S_i = g \times S_{i-1}$. For the noise component, the classic formulae which expresses the output noise of a combination of two successive phenomena (see [13], [14]) is: $\sigma_i^2 = N_{i-1} \cdot \sigma_g^2 + g^2 \cdot \sigma_{i-1}^2$, where precisely, the term $g^2 \cdot \sigma_{i-1}^2$ represent the effect of the gain on the previous noise while $N_{i-1} \cdot \sigma_g^2$ is the effect of the variance of the gain on the previous mean component. As we work with noise image and not the noise variance image and because the noise can be reasonably assumed to be Gaussian (large number of quanta), the final noise image is finally computed with a random number generator, according: $N_i = \text{Gaussian noise (mean} = g \times N_i, \text{variance} = N_{i-1} \cdot \sigma_g^2)$.

- Deterministic spreading process

A deterministic spreading process is characterized by its MTF which is defined in the frequency space. Precisely, the MTF is the module of the Fourier transform of the Point Spread Function (PSF). In most cases of isotropic systems, the phasis of the Fourier transform of the PSF is null. In opposition to a stochastic spreading, a deterministic spreading is a process which transforms data in an entirely determined way, without statistic uncertainty. Thus, transform formulae are : $S_i = S_{i-1} \circ \text{PSF}$ and $N_i = N_{i-1} \circ \text{PSF}$. Of course, practically, convolutions will be substituted by multiplications by the MTF in the frequency domain.

- Stochastic spreading process

As the deterministic spreading process, the stochastic spreading is characterized by its MTF, or PSF. The difference is that PSF is interpreted as a probability law to apply for each quanta of the initial image. Consequently, no analytical formulae can be expressed for the transformation of mean and noise images. Cunningham and co ([14]) has introduced a new symbol $*_s$ to represent mathematically this stochastic spreading. Monte Carlo algorithms are the most adapted to model stochastic phenomena. In this case, it would

consist in using randomised numbers, according to PSF, for each quantum of the initial mean and noise images. For that, times of calculation of such algorithms are very long. However, as demonstrated in [18], stochastic spreading seems deterministic if the number of quanta by pixels is large enough (>1000). In our case (source X for CND applications), the number of photons by pixel is always superior. Consequently, in most cases, the deterministic spreading will be preferred to speed up the calculation.

- Noise addition process

The noise addition process is only characterized by the standard deviation of the noise which is added, considering that it is a gaussian noise. Of course, the mean image do not change. Concerning the noise image, it has to be generated on the previous noise image. So, equations are: $S_i = S_{i-1}$ and $N_i = \text{Gaussian noise (mean = } N_i, \text{ variance = } \sigma_g^2)$.

- Non linear conversion process

The user has also the possibility to identify an eventual non linearity process in the detector, called “non linear conversion”. In a flat panel, a non linear conversion will be modelled for the last conversion of the electronics which is the transformation of the electronic signal in grey levels. It is carried out thanks to a simple conversion table, which is interpolated for any input value.

4.3 Validation on a scintillator screen with an *a*-Si photosensor matrix

This cascaded system model has been validated with two different flat panels: the FLASHSCAN 35 and the DXR500 ([12], Deliv.1.16). We present here the validation performed on a peculiar flat panel, derived from the FLASHSCAN 35, with a simple wedge in TA6V (titanium alloy), which thickness is 2mm and in which several well dimensioned flaws have been included (flat bottom holes, half sphere impact, rectangular cracks) (figure 7). The X-ray tube delivers X-ray beams of 150 kV with appropriate filters (2mm copper + 2mm steel) during 3.16s and with an intensity of 3 mA. The source focus is large (about 1mm) and so not well adapted to the detection of such small defects. However, this simulation presents a first interesting case for global validation of Sindbad with flat panel detectors and well dimensioned flaws.

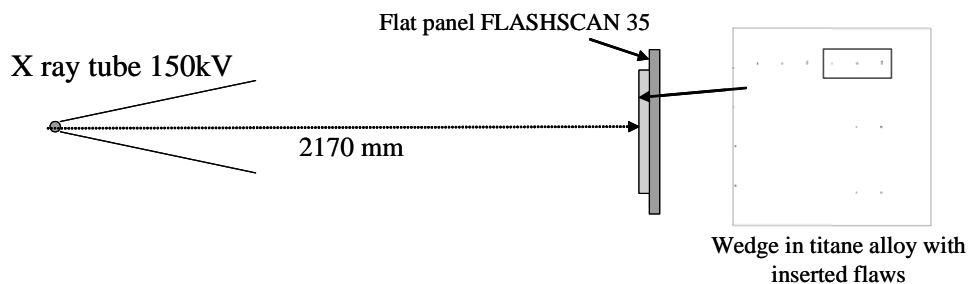


Figure 7 : Experimental bench for validation

Our customized FLASHSCAN flat panel detector is composed of 350 μm of $\text{Gd}_2\text{O}_2\text{S:Tb}$ coupled to a grid of amorphous silicon photodiodes. The pixel size is 0.127x0.127 μm and the signal is coded on 14 bits. 8 various elementary physical processes can be identified to describe this flat panel according to the cascaded linear system model (Table 1).

Table 1: List of the successive elementary processes identified for the case of the FLASHSCAN 35.

Title of step	Type of process	Unity
0. Primary detection of x rays quanta in the detector	Interaction	absorbed energy (keV)
1. Secondary detection of x rays	Stochastic spreading	absorbed energy (keV)
2. Conversion to light quanta	Amplification	keV => optical photons
3. Scattering of light quanta in scintillator	Stochastic spreading	optical photons
4. Escaping of light quanta	Amplification	optical photons
5. Collection of light quanta on photodiodes surface	Amplification	optical photons
6. Detection of optical quanta in photodiodes	Amplification	optical photons => e ⁻
7. Addition of electronic noise	Noise addition	electrons
8. Conversion in grey levels	Conversion	electrons => grey levels

The model used for this flat panel is inspired by the one proposed by Bissonnette ([15],[16],[17]) in case of portal imaging. Each step has been characterized by parameters determined either by constructor characteristics (filling factor), experimental measurements (final conversion step), literature data (light quanta energy and escaping factor in Gd₂O₂S:Tb, light quantum efficiency of photodiodes), analytical models (Swank model for light spread MTF) or even pre simulations (interaction MTF estimated by Monte Carlo simulation). This study has been lead under the Verdict project and details of all parameters chosen for each step are available in [12], Deliv.1.16.

Figure 8 shows the experimental and simulated images of the wedge, focusing on the biggest rectangular cracks. Dimensions of these cracks are for (a): length = 1 mm, depth = width = 0.2mm, (b): length = 1 mm, depth = width = 0.5mm and (c): length = 2 mm, depth = width = 0.5mm. Visually, the experimental image is quite similar to the image simulated with Sindbad. The level of detectability is the same: experimentally or after simulation, the two biggest cracks are easily detectable whereas it looks difficult but possible for the smallest one. This is confirmed with the profiles. However, it seems that the noise has been over estimated in simulation. This can be due to an under estimated MTF or an over estimated electronic noise. Corrections of these parameters should be done to improve the agreement between simulation and experiment.

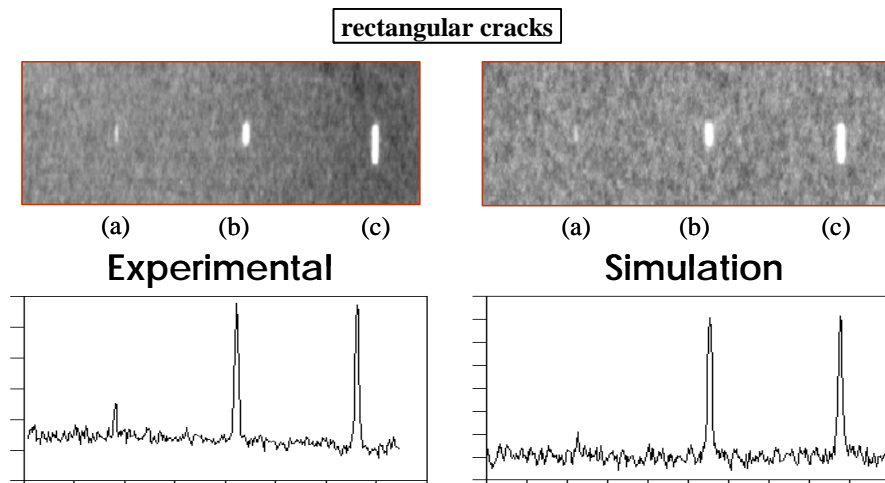


Figure 8 : Comparison of experimental and simulated images obtained on rectangular cracks

5. Conclusion

Several new developments have been achieved in the X-ray radiographic simulation software Sindbad to improve its performances for realistic x-ray simulation devoted to complex parts inspection. Concerning scattered modelling, the Monte Carlo code has been accelerated in cases of low stopping power detectors. Thanks to BRL-CAD interface, many defects can be easily inserted in complex parts and taken into account in Sindbad simulations thanks to an automatic over sampling of the detector. Finally, concerning detector simulation, the new version of Sindbad proposes a new model: the cascaded system model. This new model enables the user to build its own detector by cumulating several linear processes for each physical phenomenon involved in the detection. It appears very powerful but requires a very good knowledge of the detector. This model has been validated with success on a flat panel detector.

Acknowledgments: This work has been partly funded by the European Commission under the 5th PCRD programme No. G4RD-CT-2002-00860 (Verdict). The authors would like to thank the Verdict partners and specially Snecma and Turbomeca for providing their industrial part models.

References

- [1] G-R. Tillack, C. Nockemann and C. Bellon, "X Ray Modelling of Projection For Industrial Applications", *NDT &E International* 33, pp 481-488, 2000.
- [2] M. Mangard, P. Hammersberg and M. Sandborg "Modelling of an X-ray Image Intensifier Based Radiography System", *J. X-ray Sci and Tech* 8, pp 31-50, 1998.
- [3] P. Duvauchelle, N. Freud, V. Kaftandjian, G. Peix, D. Babot, "Development of a simulation tool for X-ray imaging techniques", Workshop on the application of X-ray tomography in materials science, Villeurbanne, Oct. 28-29, 1999, ed. by J. Baruchel et al., Hermes, Paris, 2000.
- [4] Bonin, B. Lavayssiere and B. Chalmond, "Moderato : A Monte-Carlo Radiographic Simulation", *Review of Progress in QNDE*, Vol 19A , pp 651-656, 1999.
- [5] F. Inanc and J. N. Gray, "A CAD Interfaced Simulation Tool for X-Ray NDE Studies", *Review of Progress in QNDE*, Vol.9, ed. by D. O. Thompson and D. E. Chimenti, Plenum Publishing Co., 1990.
- [6] R. Guillemaud, J. Tabary, P. Hugonnard, F. Mathy, A. Koenig, A. Glière, "Sindbad : a multi-purpose and scalable X-ray simulation tool for NDE and medical imaging", PSIP 2003, Grenoble, France, 2003.
- [7] J. Tabary and A. Glière, "Coupling photon Monte Carlo simulation and CAD Software. Application to X-ray nondestructive evaluation," in *Proc. Monte Carlo 2000*, pp 461-466, Lisbon, Portugal, Oct. 23-26, 2000.
- [8] J. Tabary, A. Glière, R. Guillemaud, P. Hugonnard, F. Mathy, « Combination of high resolution analytically computed uncollided flux images with low resolution Monte Carlo computed scattered flux images", *IEEE Transactions on Nuclear Science*, Vol. 51, No. 1, pp 212-217, Feb 2004.
- [9] J. Tabary, P. Hugonnard, F. Mathy, R. Guillemaud, "Recent improvements for scatter simulation in Sindbad, a coupled photon Monte Carlo and CAD software", *Proc. WCNDT*, Montreal, Sept. 2004.
- [10] P.C. Dykstra, M.J. Muus, "The BRL-CAD package: An overview," in *Proc. 4th Computer Graphics Workshop--USENIX*, Phoenix, Arizona, U.S., pp 73-80, Oct. 1987. Available : <http://www.brlcad.org/>
- [11] J.C. Satterthwaite, "EGSNova : An adaptation of EGS in C/C++," May 1998. [Online]. Available : <http://www.nemc.org/nova>.
- [12] Deliverables of Verdict project, especially Deliv.1.7 (intern ref. 2005-65), Deliv.1.10 (intern ref. 2005-64), and Deliv.1.16 (intern ref. 2006-22).
- [13] M. Rabani, R. Van Matter "Analysis of signal and noise propagation for several imaging mechanisms ", *J. Opt. Soc. Am.*, Vol 6, n°8, pp 1156-1164,1989.
- [14] I.A. Cunningham, M.S. Westmore, A. Fenster "Effect of finite detector element with on the spatial-frequency-dependent Detective Quantum Efficiency", *SPIE Vol. 2432*, pp143-151, 1995.
- [15] J.P.Bissonnette, I.A.Cunningham, P.Munro : "Optimal phosphor thickness for portal imaging", *Med. Phys.* 24 (6), pp 803-813, 1997.
- [16] J.P.Bissonnette, I.A.Cunningham, D.A. Jaffray, A. Fenster, P.Munro : "A quantum accounting and detective quantum efficiency analysis for video-based portal imaging", *Med. Phys.* 24 (6), pp 815-825, 1997.

- [16] J.P.Bissonnette, P.Munro, I.A.Cunningham: "Monte Carlo of the image formation process in portal imaging", Med. Phys. 30 (12), pp 3243-3250, 2003.
- [18] J.P.Moy: "Signal-to-noise ratio and spatial resolution in x-ray electronic imagers: Is the MTF e relevant parameter?", Med. Phys. 27 (1), pp 86-93, 2000.